Available online at www.sciencedirect.com

SCIENCE DIRECT®

Journal of Molecular Catalysis A: Chemical 255 (2006) 269–274

JOURNAL OF MOLECULAR CATALYSIS A: CHEMICAL

www.elsevier.com/locate/molcata

Racemization of *R*-2-amino-1-butanol catalyzed by a fixed-bed Raney cobalt catalyst

Yuecheng Zhang[a], Guoyi Bai[b], Yang Li[a], Xilong Yan[a], Ligong Chen[a,*]

[a] *School of Chemical Engineering and Technology, Tianjin University, Tianjin 300072, PR China*
[b] *College of Chemistry and Environmental Science, Hebei University, Baoding 071002, PR China*

Received 26 June 2005; received in revised form 12 April 2006; accepted 13 April 2006
Available online 22 May 2006

Abstract

Racemization of *R*-2-amino-1-butanol proceeded effectively over a fixed-bed Raney cobalt catalyst in a continuous fixed-bed reactor under the hydrogen pressure in the range of 2.0–6.0 MPa. The performance of a fixed-bed Raney cobalt catalyst was compared with that of a pulverous Raney cobalt catalyst. The catalysts were characterized by X-ray photoelectron spectroscopy (XPS), X-ray diffractometry (XRD), environment scanning electron microscopy (ESEM) and N_2 adsorption measurement (BET). The activity and stability of the fixed-bed Raney cobalt catalyst and the effects of concentration, temperature and hydrogen pressure were examined. Racemic 2-amino-1-butanol was obtained with a total yield of over 76% under the optimum reaction conditions. Thus, an effective process for the racemization of *R*-2-amino-1-butanol has been established.

Keywords: Racemization; Raney cobalt catalyst; 2-Amino-1-butanol

1. Introduction

S-2-amino-1-butanol is a key intermediate for the synthesis of ethambutol hydrochloride, which is an important anti-tuberculosis agent [1,2]. Most processes for the synthesis of 2-amino-1-butanol produce racemic 2-amino-1-butanol [3–8]. Enantiomerically pure *S*-2-amino-1-butanol can then be obtained through the resolution of racemic 2-amino-1-butanol [9]. The unwanted *R*-2-amino-1-butanol is converted back to the racemate for recycling. In other studies, the racemization of *R*-2-amino-1-butanol required ammonia, and cannot be readily adapted to a continuous process [10–12].

Raney catalysts are used mainly in the powdered form in a large number of reactions, such as hydrogenation, dehydrogenation, isomerization and hydration [13]. Powdered catalysts can only be used in a batch process and have to be separated from the reaction medium after the reaction [14]. To overcome this limitation, a variety of methods for preparing fixed-bed Raney catalysts have been reported [15–19].

In this paper, the catalytic racemization of *R*-2-amino-1-butanol was studied in a continuous fixed-bed reactor under the hydrogen pressure in the range of 2.0–6.0 MPa. Differences between a fixed-bed Raney cobalt catalyst and a pulverous Raney cobalt catalyst were studied by X-ray photoelectron spectroscopy (XPS), X-ray diffractometry (XRD), environment scanning electron microscopy (ESEM) and N_2 adsorption (BET) methods. In addition, the catalytic activity and stability of this Raney Co Catalyst for the racemization of *R*-2-amino-1-butanol was studied, and the reaction parameters were optimized.

2. Experimental

2.1. Materials and catalysts

Co–Al alloy was purchased from Jinzhou Catalyst Factory, Jinzhou, China. *R*-2-amino-1-butanol, 99%, was obtained from Xinxiang Jujing Chemical Limited Company, Xinxiang, China. Commercially available solvents and reagents were used without further purification.

The Raney cobalt catalyst was prepared by kneading a mixture of the alloy and an assistant as described previously [19]. Powdered Co–Al alloy, with a nominal compositions of Co (40) Al (60), together with poly(vinyl alcohol) (molecular

---

* Corresponding author. Tel.: +86 22 27891034; fax: +86 22 27406314.
E-mail address: lgchen@tju.edu.cn (L. Chen).

1381-1169/$ – see front matter © 2006 Elsevier B.V. All rights reserved.
doi:10.1016/j.molcata.2006.04.033

weight = 5000) and water were mixed, and the mixture was then kneaded for 3 h. The material was extruded in bars of 1–2 mm diameter and a length of 3–4 mm. The extrudates were then dried at 120 °C for 12 h, followed by caclination at 750 °C for 1 h and then at 900 °C for 2 h. After calcination, the alloys were activated in a 20 wt.% NaOH solution for 26 h at 90 °C. Finally the catalyst was washed thoroughly with distilled water and stored in distilled water.

The pulverous Raney Co catalyst was prepared as described in the literature [12]. The powdered Co–Al alloy (40/60) was activated in a 5 wt.% NaOH solution at 35 °C, activation being continued until about 35% of the original Al in the alloy was removed. Finally the catalyst was washed thoroughly with distilled water and stored in distilled water.

2.2. Catalyst characterization

XPS measurements were recorded with a Phi 1600 spectrometer using an Mg Kα X-ray source for excitation. Electron micrographs were obtained using a XL30 environment scanning electron microscope (ESEM). XRD spectra were recorded on a D/max 2500 X-ray diffractometer with Cu Kα radiation. Surface area (BET) measurements were performed at 77 K on a Micromeristics ASAP 2010 sorptometer.

2.3. Racemization procedure

Racemization of *R*-2-amino-1-butanol with the fixed-bed catalyst was carried out in a tubular, fixed-bed reactor with an inner diameter of 15 mm and a length of 1100 mm. The reactor was loaded with 20.0 g of fixed-bed Raney cobalt catalyst. A solution of *R*-2-amino-1-butanol in dioxane was dosed into the reactor at a speed of 1 mL/min by a syringe pump. The temperature in the reaction zone was measured with a thermocouple located in the center of the tube and was regulated by a PID cascade controller. The hydrogen pressure in the reaction system was set by a Tescom back pressure regulator. The reaction mixtures were collected and distilled to give racemized 2-amino-1-butanol. The reaction mixtures were analyzed by GC–MS using a 25 m SE-54 capillary column and the optical rotation data were obtained by a WZZ-3 auto-rotation analyzer.

Racemization of *R*-2-amino-1-butanol with the pulverous and fixed-bed Raney Co catalysts were carried out in a stainless steel autoclave. The reaction mixtures were collected and analyzed as described above.

2.4. Data analysis

The performance of the catalysts was estimated by calculating the conversion and the recovery for the racemization of *R*-2-amino-1-butanol.

The conversion was based on the optical rotation, [α]. The conversion is given by

$$(1 - [\alpha]_{\text{product}}/[\alpha]_{\text{material}}) \times 100\%$$

where $[\alpha]_{\text{product}}$ is the optical rotation of the product and $[\alpha]_{\text{material}}$ is the optical rotation of the starting material.

The recovery of 2-amino-1-butanol is given by

$$(w_{\text{product}}/w_{\text{material}}) \times 100\%$$

where w_{product} is the amount of 2-amino-1-butanol after the reaction and w_{material} is the amount of 2-amino-1-butanol used in the reaction.

3. Results and discussion

3.1. Catalyst characterization

Raney Co has been shown to be an effective catalyst for the racemization of amino alcohols [12]. Partial results for the racemization of *R*-2-amino-1-butanol using a fixed-bed Raney Co catalyst and pulverous Raney Co catalyst are given in Table 1.

The experimental results showed that the racemization proceeded more effectively with the fixed-bed Raney Co catalyst; furthermore the fixed-bed Raney Co catalyst can be readily adapted to a continuous process. In order to better understand these results, the catalysts were characterized by XPS, XRD, SEM and BET.

Table 1
Results of different catalysts for the racemization of *R*-2-amino-1-butanol

Entry	Temperature (°C)	Hydrogen pressure (MPa)	Recovery ratio (%)	Conversion ratio (%)	Total yield (%)
1[a]	160	3.0	84.3	86.7	73.1
2[a,b]	160	3.0	81.9	90.2	73.8
3[a]	180	3.0	79.2	91.2	72.2
4[a]	160	5.0	88.3	83.1	73.4
5[c]	160	5.0	89.2	85.5	76.3
6[a]	180	4.0	80.4	90.5	72.8
7[c]	180	4.0	79.0	94.5	74.6
8[d]	160	3.0	87.6	93.2	81.6

[a] Reaction conditions: reactor stainless steel autoclave; catalyst, 5.00 g pulverous Raney Co; *R*-2-amino-1-butanol, 50 g; solvent, dioxane; volume, 50 mL; reaction time, 3 h.

[b] Reaction time, 6 h.

[c] Reaction conditions: reactor stainless steel autoclave; catalyst, 5.00 g fixed-bed Raney Co; *R*-2-amino-1-butanol, 50 g; solvent, dioxane; volume, 50 mL; reaction time, 3 h.

[d] Reaction conditions: reactor fixed-bed reactor; catalyst, fixed-bed Raney Co; concentration of the solution, 20%; solvent, dioxane; flow rate, 1 mL/min; the samples were taken after 5 h of time on stream.

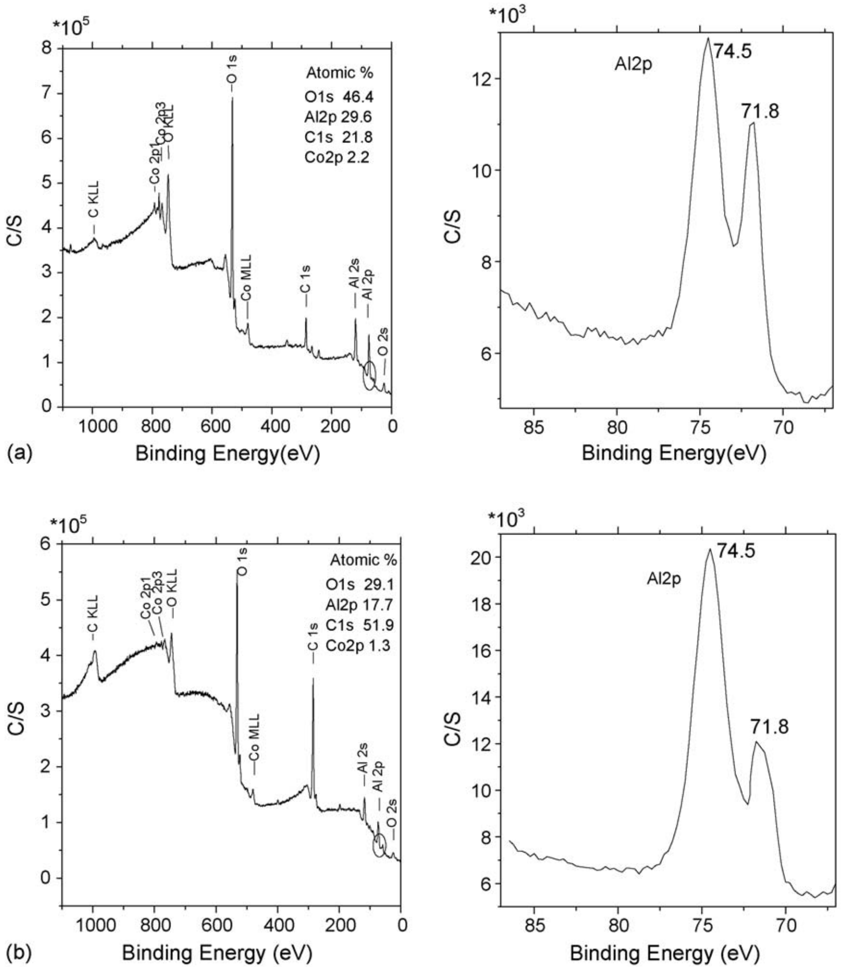

Fig. 1. XPS spectroscopy of: (a) the Co–Al alloy and (b) the calcined Co–Al alloy.

Fig. 1 shows the XPS spectra for the powdered Co–Al alloy and the calcined Co–Al alloy. An XPS peak with a binding energy of 778.4 eV was observed for the Co $2p_{3/2}$ level, and can be assigned to elemental cobalt on the surface of the sample [20]. The binding energy of the Co $2p_{3/2}$ level is the identicals in the two XPS spectra, which indicates that Co was not been oxidized during the calcination process. However, the aluminum species are present in two states. The peaks at 71.8 and 74.5 eV can be assigned to elemental Al and oxidized Al, respectively. After the calcination, the proportions of these two peaks areas changed, indicating that some Al was oxidized to α-Al_2O_3 during the heating. The surface compositions of the samples calculated by analysis of the relative XPS peaks area were $Al_{37.4}Co_{2.8}O_{58.6}$ for the alloy and $Al_{36.8}Co_{2.7}O_{60.5}$ for the calcinated sample. This result also supports the above conclusion.

XRD analysis was used to identify the bulk phases in the fixed-bed and pulverous Raney Co catalysts. The diffraction patterns are shown in Fig. 2. A great abundance of the Co phase was detected in both catalysts, and the Co phase peaks were broader than normal Co phases, which indicates that some of the metallic Co is present in the amorphous state. Peaks for α-Al_2O_3 were also found in the XRD pattern of the fixed-bed Raney Co catalyst. These peaks are attributed to α-Al_2O_3 formed during

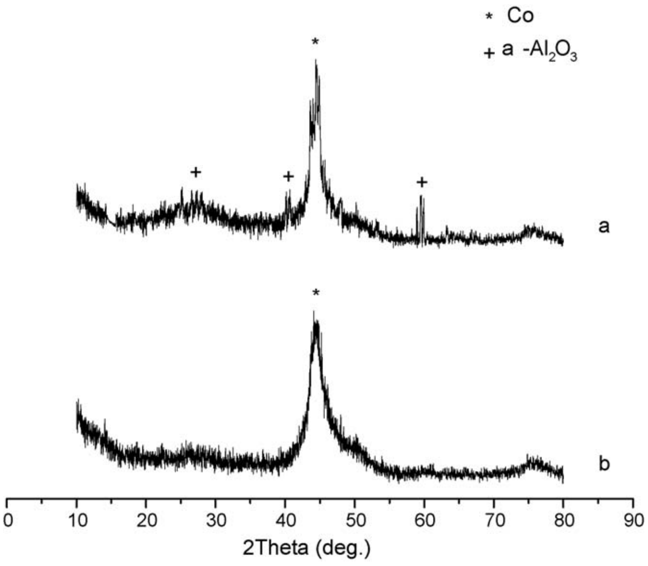

Fig. 2. XRD patterns of: (a) the fixed-bed Raney Co catalyst and (b) the pulverous Raney Co catalyst.

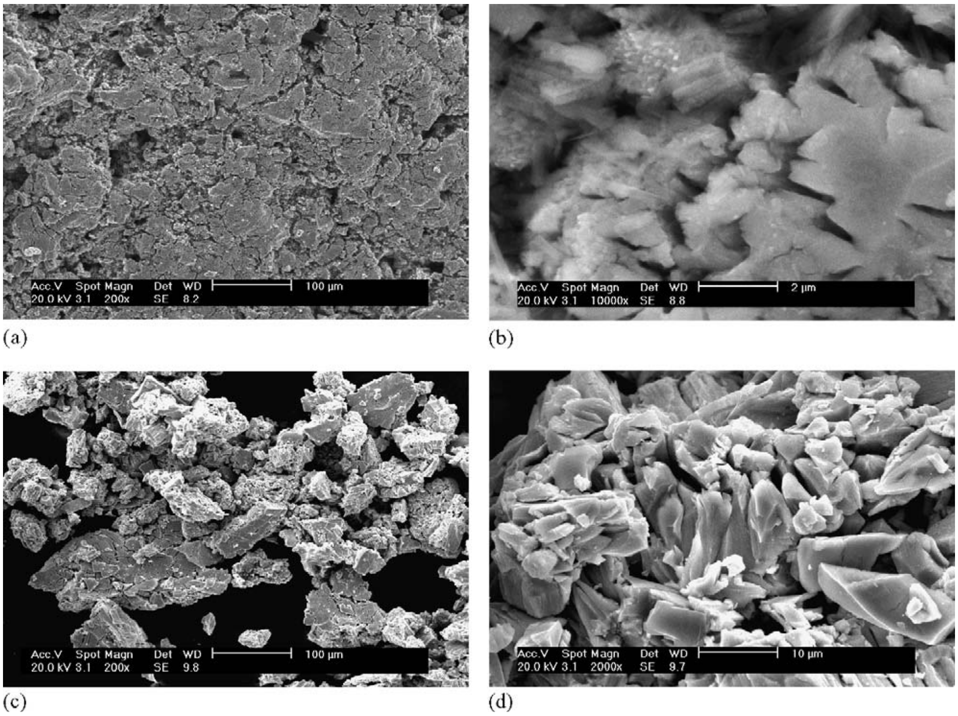

(a) (b) (c) (d)

Fig. 3. SEM micrographs of the fixed-bed Raney Co catalysts: (a) ×200 and (b) ×10,000; the pulverous Raney Co catalyst: (c) ×200 and (d) ×2000.

calcination, which are not dissolved by the NaOH solution during the catalyst activation step.

The surface morphologies of the two kinds of Raney Co catalysts were characterized by SEM. Typical SEM pictures of the spongy feature of the samples are shown in Fig. 3. The pulverous catalyst has particles sizes ranging from 1 to 100 μm with irregular and undefined shapes. The surface of the fixed-bed catalyst contains some micropores with diameters smaller than 20 μm, which is one of the main characteristics of the fixed-bed Raney catalysts [21]. The surface also contains particles of α-Al_2O_3 which were identified by EDS analyses.

BET measurements gave the surface area, pore volume and average pore diameter of the catalysts. The results are given in Table 2 and the distribution of pore size is shown in Fig. 4. The surface area and pore volume of the pulverous Raney Co catalyst are 91.9 m^2/g and 0.26 cm^3/g, respectively, which are both larger than those of the fixed-bed Raney catalyst. However, the average pore diameter of the fixed-bed Raney Co catalyst is larger than the pulverous Raney Co catalyst, which is also evident from the distribution of the pore sizes of these catalysts. Large pores facilitate the fast diffusion of substrates to the active center, which can increase the catalytic activity of the fixed-bed Raney Co catalyst.

From the combined results of XPS, XRD, SEM and BET, two conclusions can be drawn: first, some of Al was oxidized to α-Al_2O_3 during the calcination process, which improves the strength and attrition resistance of the fixed-bed Raney cobalt catalyst [19]. Therefore the fixed-bed Raney Co catalyst can be readily adapted to a continuous process in a fixed-bed reactor. Second, the fixed-bed Raney Co catalyst contains some micropores and the average pore diameter of this catalyst is larger

Table 2
N_2 adsorption results of the fixed-bed Raney Co catalysts and the pulverous Raney Co catalysts

Entry	Catalyst	Surface area[a] (m^2/g)	Pore volume[b] (cm^3/g)	Average pore diameter[c] (Å)
1	Raney Co	91.9	0.26	112.4
2	Fixed-bed Raney Co	23.1	0.08	146.6

[a] Calculated from the BET equation.
[b] Calculated from the BJH equation.
[c] Average pore diameter = 4 × pore volume/surface area.

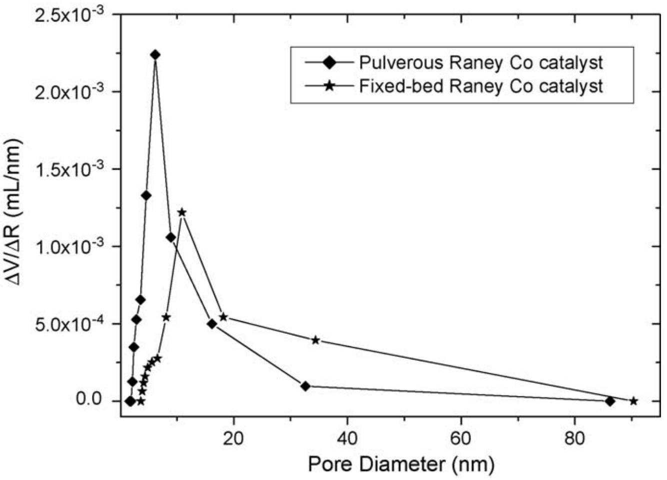

Fig. 4. Distribution of pore size of the fixed-bed Raney Co catalysts and the pulverous Raney Co catalyst.

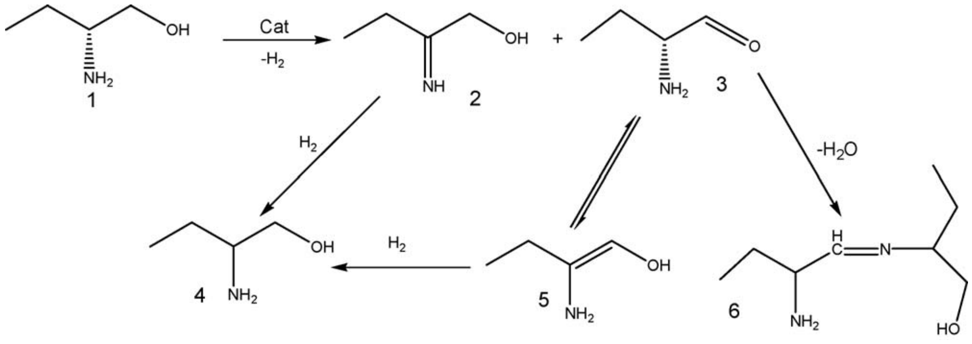

Scheme 1. Racemized pathway of *R*-2-amino-1-butanol.

than the pulverous Raney Co catalyst, which can facilitate the fast diffusion of substrates to the active center and improve the catalytic activity.

3.2. Reaction parameters

To achieve the best catalytic results, the reaction parameters, including the concentration of the *R*-2-amino-1-butanol solution, the temperature and the hydrogen pressure, were optimized.

The reaction mixtures were analyzed by GC–MS. From these results, the reaction pathway, depicted in Scheme 1, was determined. Furthermore, since the activity of the fixed-bed Raney Co catalyst for dehydrogenation is moderate and it favors the dehydrogenation of amino group, compound (**2**) is certainly the key intermediate and the pathway from compound (**1**) → (**2**) → (**4**) is the major pathway. In this reaction, the dehydrogenation of the alcohol to form the aldehyde (**3**) also occurs. The aldehyde (**3**) can then undergo a condensation with (**1**) to form by-product (**6**). Aldehyde (**3**) can also rearrange to form compound (**5**), which can then form product (**4**) via hydrogenation.

3.2.1. Effect of solution concentration

The 2-amino-1-butanol concentration was found to have a remarkable influence on the recovery but little effect on the conversion. Starting material solutions with different concentrations were examined, and the results are presented in Fig. 5. With increasing concentration, the recovery decreased. The higher concentration of 2-amino-1-butanol gives the aldehyde intermediate (**3**) more, enhancing chances to form compound (**6**) via the condensation (Scheme 1). Consequently, relatively lower concentrations produce higher recovery. Thus, 2-amino-1-butanol concentration of 20% was chosen as the optimum concentration.

3.2.2. Effect of temperature

The racemization of *R*-2-amino-1-butanol was carried out between 150 and 190 °C, and the results are displayed in Fig. 6. As the temperature increased, the conversion increased to 95% at 190 °C, but the recovery decreased. Higher temperatures promote the dehydrogenation of both the amine and the alcohol groups of compound (**1**), and thus the selectivity of the catalyst is decreased. The increase in the dehydrogenation of the alcohol group to (**3**) results in an increase in the formation of compound (**6**). Thus, according to the results in Fig. 6, 160 °C was chosen as the optimum reaction temperature.

3.2.3. Effect of hydrogen pressure

Fig. 7 shows the influence of hydrogen pressure on the reaction. The conversion ratio decreased from 93.2% to 87.2% when the hydrogen pressure increased from 2.0 to 6.0 MPa, but the recovery increased with increasing pressure. This result can be

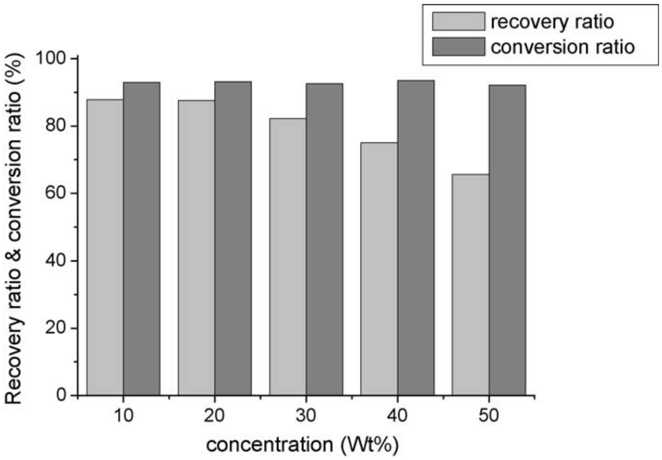

Fig. 5. Effect of solution concentration on the reaction. Reaction conditions: temperature, 160 °C; hydrogen pressure, 3.0 MPa; solvent, dioxane.

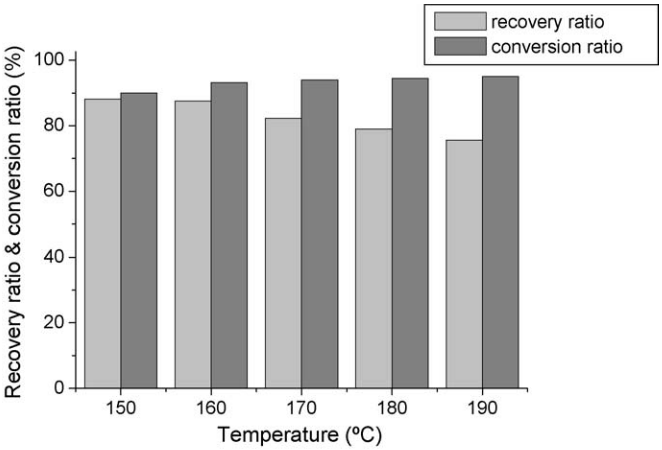

Fig. 6. Effect of temperature on the reaction. Reaction conditions: hydrogen pressure, 3.0 MPa; concentration of the solution, 20%; solvent, dioxane.

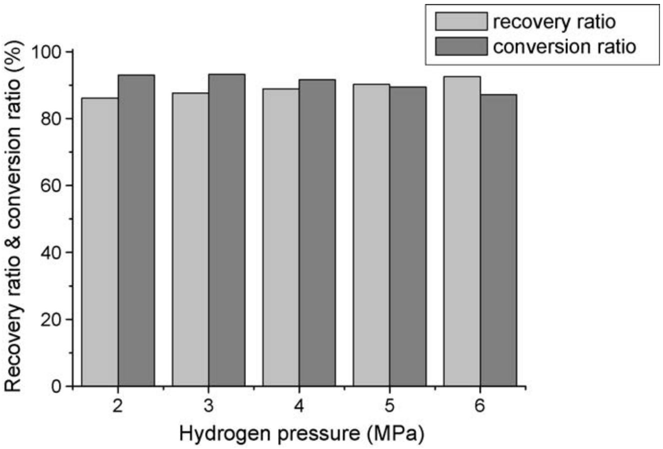

Fig. 7. Effect of hydrogen pressure on the reaction. Reaction conditions: temperature, 160 °C; concentration of the solution, 20%; solvent, dioxane.

explained by the dehydrogenation/hydrogenation nature of the reaction. A high hydrogen pressure inhibits the dehydrogenation of both the amine and the alcohol groups, so the formation of compounds (**2**) and (**3**) are decreased with increasing pressure. Since compound (**2**) is a key intermediate, the hydrogen pressure cannot be too high. Therefore, 3.0 MPa was selected as the optimum hydrogen pressure for both the conversion and feasibility of operation.

3.3. Lifetime of the fixed-bed Raney catalyst

Since a continuous process for the racemization of *R*-2-amino-1-butanol in a fixed-bed reactor was established here, the life of the catalyst was also tested. The reaction was carried out under optimum reaction conditions for over 100 h. The catalyst showed excellent stability during this period. The conversion remained in the range of 90–93% and the recovery ratio remained above 85%. Thus, the total yield of racemized 2-amino-1-butanol was over 76%. Therefore, the catalyst can be economically used in large-scale productions.

4. Conclusions

In this work, we described an effective process for the racemization of 2-amino-1-butanol over a Raney Co catalyst in a fixed-bed reactor. The fixed-bed Raney Co catalyst contains some α-Al_2O_3 and has some micropores. The average pore diameter of this catalyst is larger than the pulverous Raney Co catalyst, which improves the catalytic activity. This catalyst shows better activity and stability than the pulverous Raney Co catalyst. Its excellent performance makes the process not only economically viable but also applicable to large-scale reactions.

Acknowledgements

The authors thank professor Q.H. Wan for his helpful suggestions. Financial support by the National Natural Science Foundation of China (Grant no. 20376057) and the Science Project of the Hebei Education Department (grant 2005350) are gratefully acknowledged.

References

[1] J. Kazan, B. Township, S. County, US Patent 3,769,347 (1973).
[2] R.G. Wilkinson, R.G. Shepherd, J.P. Thomas, C. Baughn, J. Am. Chem. Soc. 83 (1961) 2212.
[3] C. Belzecki, W. Tomasik, J. Trojoar, US Patent 3,953,512 (1976).
[4] T. Kamei, Y. Shimasaki, H. Tsuneki, K. Yamamoto, Y. Morimoto, M. Ueshima, US Patent 4,966,980 (1990).
[5] B. Singh, US Patent 3,944,617 (1976).
[6] J.B. Tindall, US Patent 3,651,144 (1972).
[7] Y. Ichikawa, E. Yoshisato, K. Nakagawa, US Patent 4,151,204 (1979).
[8] L. Bernardi, M. Foglio, A. Temperili, US Patent 3,847,991 (1974).
[9] N.W. Fadnavis, M. Sharfuddin, S.K. Vadivel, Tetrahedron: Asymmetry 10 (1999) 4495.
[10] R. Potarraju, H.M. Vishnu, Indian Patent 162213 (1988).
[11] Y. Ichikawa, K. Nakagawa, E. Yoshisato, US Patent 4,096,186 (1978).
[12] S.G. Harsy, US Patent 4,990,666 (1991).
[13] P. Fouiloux, Appl. Catal. 8 (1983) 1.
[14] W.C. Cheng, L.J. Czarnecki, C.J. Pereira, Indust. Eng. Chem. Res. 28 (1989) 1764.
[15] M.B. Sherwin, S.P. Wang, S.R. Montgomery, US Patent 4,721,811 (1988).
[16] B. Breitscheidel, U. Diehlmann, T. Rühl, S. Weiguny, US Patent 6,121,188 (2000).
[17] P. Schuetz, R. Burmeister, B. Despeyroux, H. Moesinger, H. Krause, K. Deller, US Patent 5,536,694 (1996).
[18] D. Ostgard, M. Berweiler, S. Röder, US Patent 6,486,366 (2002).
[19] M. Vicari, K. Flick, J.P. Melder, W. Schnurr, J.W. Döring, US Patent 5,733,838 (1998).
[20] H. Li, Y. Wu, H. Luo, M. Wang, Y. Xu, J. Catal. 214 (2003) 15.
[21] H.J. Zhao, R. Bai, C.G. Liu, Modern Chem. Indust. 24 (11) (2004) 15.